

# Towards an understanding of CMR pyrochlore $\text{Tl}_2\text{Mn}_2\text{O}_7$

C.I. Ventura \*

*Centro Atómico Bariloche, 8400 - Bariloche, Argentina*

M.A. Gusmão

*Instituto de Física, Universidade Federal do Rio Grande do Sul, CP 91501-970 Porto Alegre, RS,  
Brazil*

## Abstract

The colossal magnetoresistance (CMR) exhibited by the pyrochlore compound  $\text{Tl}_2\text{Mn}_2\text{O}_7$  was discovered in 1996. Important differences with CMR Mn-perovskite compounds regarding crystal structure and electronic properties were soon realized, indicating the possibility of different mechanisms for CMR being present. Recently, new pyrochlore compounds exhibiting CMR were prepared. The larger experimental background now existent, has received diverse interpretations. In the present work, we aim to contribute to the understanding of the properties of  $\text{Tl}_2\text{Mn}_2\text{O}_7$  through the study of a generic model for the compound, including Hund and superexchange couplings as well as hybridization effects (HS model). The model includes two kinds of electronic orbitals, as widely believed to be present: one, directly related to the magnetism of the compound, involves localized Mn moments, represented by spins, and a narrow band strongly Hund-coupled to them. Also, more extended electronic orbitals, related to the carriers in  $\text{Tl}_2\text{Mn}_2\text{O}_7$ , appear and hybridize with the narrow band. The possibility of a superexchange coupling between the localized spins is also allowed for. This generic model allows exploration of many of the proposals put forward by other researchers for

Tl<sub>2</sub>Mn<sub>2</sub>O<sub>7</sub>. As a first approach to the problem, here we employ a mean field approximation to study the magnetic phase-diagram and electronic structure of the HS model, for various sets of parameters mentioned before in connection with the compound. Furthermore, we are able to exhibit similarities with predictions obtained in 1997 using an intermediate valence model for Tl<sub>2</sub>Mn<sub>2</sub>O<sub>7</sub>, if appropriate sets of parameters are used. In particular, we show here many common features which can be obtained for the electronic structure around the Fermi level in the ferromagnetic phase. Due to the simplifications adopted in the present treatment the comparison between the models could not be extended to higher temperatures here.

75.30.Vn,75.50.-y,75.30.Et,71.20.-b,71.27.+a

## I. INTRODUCTION

Since its discovery in 1996,<sup>1-3</sup> the colossal magnetoresistance (CMR) exhibited by the pyrochlore compound  $\text{Ti}_2\text{Mn}_2\text{O}_7$  posed many interesting questions. First among them, whether a common fundamental mechanism could be responsible for the origin of CMR both in this compound and in the larger family of perovskite manganese oxides,<sup>4</sup> which have different crystal structure and electronic properties. The recent appearance of CMR in other compounds with the pyrochlore crystal structure<sup>5,6</sup> exhibiting long range ferromagnetic ordering, and the larger experimental background now existent, allow a better standpoint to approach the theoretical description of this compound.

$\text{Ti}_2\text{Mn}_2\text{O}_7$  undergoes a ferromagnetic transition with critical temperature<sup>2,6</sup>  $T_c \sim 125\text{K}$  (also reported<sup>1,3</sup> as  $140\text{K}$ ), below which temperature the compound exhibits long range ferromagnetic ordering and is metallic. A sharp decrease in resistivity with the development of spontaneous magnetization below  $T_c$ , and the magnetoresistance maximum around  $T_c$  with field induced magnetization, which are similar to those of CMR Mn-perovskites, indicate that a strong coupling between transport and magnetism also exists in  $\text{Ti}_2\text{Mn}_2\text{O}_7$ .<sup>1-3</sup> But important differences have been established with respect to the CMR perovskites, starting from its  $\text{A}_2\text{B}_2\text{O}_7$  “pyrochlore” crystal structure.<sup>7</sup> No  $\text{Mn}^{3+}$  has been detected,<sup>1,3,8</sup> so that the associated Jahn-Teller structural distortions<sup>9</sup> as well as a possible double exchange (DE) mechanism<sup>10</sup> inducing ferromagnetism between  $\text{Mn}^{3+}$ - $\text{Mn}^{4+}$  pairs, studied in connection with CMR in perovskite manganites,<sup>4,9</sup> are absent. The crystal structure is almost temperature independent around  $T_c$ , no structural anomalies appear which could be associated with the change in magnetotransport properties, thus evidencing negligible spin-lattice correlations.<sup>1</sup> Structural analysis indicate negligible O deficiencies present<sup>3</sup> in stoichiometric  $\text{Ti}_2\text{Mn}_2\text{O}_7$ , and recently specially synthesized  $\text{Ti}_{2-x}\text{Mn}_2\text{O}_{7-y}$  defect compounds show the development of spin-glass behavior subjacent to ferromagnetism.<sup>11</sup> Magnetization measurements for the stoichiometric compound have shown saturation values of e.g.  $\mu_S \sim 2.59$ ,<sup>1</sup>  $2.7$ ,<sup>3,12</sup>  $2.8$ ,<sup>13</sup>  $3 \mu_B$ ,<sup>6</sup> which are in general slightly lower than the  $3\mu_B$  expected for  $\text{Mn}^{4+}$

ions with a  $3d^3$  ( $S = 3/2$ ) configuration. Hall experiments have indicated a very small number of high mobility electron-like carriers:  $\sim 0.001$ - $0.005$  conduction electrons per formula unit,<sup>3,14</sup> differing notably with the hole-doped Mn-perovskites where CMR appears around 30% doping. The critical temperature  $T_c$  has been reported to show a negative pressure dependence,<sup>5</sup> again in contrast to CMR perovskites, though above 10 Kbar a change of tendency and positive pressure shifts of  $T_c$  in  $\text{Tl}_2\text{Mn}_2\text{O}_7$  have been reported.<sup>15,16</sup> Recently, also striking differences with the perovskites were reported for the evolution of the charge dynamics probed in optical conductivity measurements.<sup>17</sup> Experimental research of magnetotransport has also been actively pursued in other pyrochlore compounds where the ordered phase remains insulating,<sup>5,6</sup> as well as in many obtained by substitutional doping of the diverse components of  $\text{Tl}_2\text{Mn}_2\text{O}_7$ .<sup>2,13,12,18,19,11,20</sup>

The experimental results have received various interpretations and prompted different proposals and suggestions for the mechanism potentially involved in CMR in  $\text{Tl}_2\text{Mn}_2\text{O}_7$  since 1996. Already in Refs. 3 and 13 it was suggested that magnetism and transport seemed related primarily to two different subsystems, unlike DE invoked for CMR perovskites: magnetism (suggested to be possibly driven by superexchange<sup>1,3</sup>) involving mostly Mn- $3d$  and O orbitals, while transport would be mainly determined by carriers involving highly itinerant Tl- $6s$  orbitals mixed with oxygen.<sup>3</sup> Unusually large scattering from spin fluctuations accompanying the FM ordering in the presence of low carrier densities was suggested as explanation for CMR.<sup>3,13</sup> Electronic structure calculations<sup>21</sup> for  $\text{Tl}_2\text{Mn}_2\text{O}_7$  indicated that the bands immediately below the Fermi level correspond mainly to Mn- $t_{2g}$  states, above the Fermi level appear Tl- $6s$  bands, while O states are mixed with these around the Fermi level. The band structure calculation by Singh<sup>22</sup> obtained a strong spin differentiation in the electronic structure around the Fermi level in the ferromagnetic ground state. The majority spin Mn- $t_{2g}$ -O- $2p$  bands below the Fermi level are separated by a gap from the Mn- $e_g$  derived bands, though there is also a mixing with Tl and O states above and below the Fermi level. Thus a small near band edge Fermi surface is obtained. For the minority channel instead, a highly dispersive band with a strong admixture of Mn, Tl and O was

found around the Fermi level, leading to a metallic minority spin channel.<sup>22</sup> In Ref. 3 it was also mentioned that the Hall data could result from a small number of carriers in the Tl-6s band: assuming  $\text{Tl}_{2-x}^{3+}\text{Tl}_x^{2+}\text{Mn}_{2-x}^{4+}\text{Mn}_x^{5+}\text{O}_7$  with  $x \sim 0.005$  the data could be accounted for, indicating a very small doping into the  $\text{Mn}^{4+}$  state.<sup>1,3</sup> In 1997, this proposal was explored in terms of an intermediate valence model (IVM) for  $\text{Tl}_2\text{Mn}_2\text{O}_7$  by Alascio and one of us (C.I.V.).<sup>23</sup> Hall experiments<sup>1</sup> and CMR results<sup>1-3</sup> could be accounted for in the context of the strongly differentiated electronic structure obtained,<sup>23</sup> with temperature and magnetic field changes which allowed explanations for the drastic carrier density changes which had been observed at  $T_c$  in Hall data,<sup>1</sup> proposing the presence of a (spin-dependent) hybridization gap or pseudogap near the Fermi level. It may be mentioned that while  $\text{Mn}^{5+}$  is a rarely found oxidation state for Mn, in  $\text{Tl}_2\text{Mn}_2\text{O}_7$  it could effectively appear as a result of the strong hybridization of orbitals near the Fermi level. Furthermore, recently the presence of  $\text{Mn}^{5+}$  ions has been reported in Cd-substituted samples ( $\text{Tl}_{2-x}\text{Cd}_x\text{Mn}_2\text{O}_7$ ) together with  $\text{Mn}^{4+}$  ions,<sup>20</sup> while in a different context  $\text{Mn}^{5+}$  in a tetrahedral environment has been found to exist in  $\text{Ba}_3\text{Mn}_2\text{O}_8$ .<sup>24</sup>

In 1998, Majumdar and Littlewood<sup>25</sup> explored the scenario of spin fluctuations around  $T_c$  in presence of very low carrier densities proposed in Refs. 3 and 13, starting from the proposal of a microscopic model involving Hund and superexchange coupling,<sup>25</sup> and showing that spin polarons might form and provide an explanation for CMR. An electronic structure calculation by Mishra and Sathpathy<sup>26</sup> in 1998 shows some common features with the IVM band structure: in the FM phase they mention the presence of a free-electron-like minority spin  $\Gamma_1$  band crossing the Fermi energy with highly mobile carriers. They relate this band to Mn- $t_{2g}$  and Tl-6s orbitals hybridized with O, the Mn- $e_g$  orbitals being higher in energy. The occupied majority-spin bands consist of a Mn- $t_{2g}$ /O band, and a small pocket of very heavy holes, unimportant for transport.<sup>26</sup> They propose a ferromagnetic double exchange Hamiltonian for  $\text{Tl}_2\text{Mn}_2\text{O}_7$  with a very small number of  $\Gamma_1$  Zener carriers which align anti-parallel to the localized Mn- $t_{2g}$  spins, including a weak AF-superexchange interaction between the localized spins. Recent optical conductivity measurements<sup>17</sup> are consistent with the main

features of the electronic structure calculations mentioned.<sup>22,23,26</sup> Recently, an explanation of the origin and pressure dependence of ferromagnetism has been put forward in terms of a conventional FM superexchange model,<sup>16</sup> provided that the intra-atomic Hund interactions in oxygen are also taken into account and the empty Mn- $e_g$  orbitals hybridize with the O and Tl levels.

In this paper we aim to contribute to the understanding of CMR in  $\text{Tl}_2\text{Mn}_2\text{O}_7$  by presenting our investigation of the magnetic phase diagram and electronic structure of a generic model for the compound, which is based on the suggestions presented by many researchers proposing the presence of superexchange interactions (of either sign) between nearest neighbor  $\text{Mn}^{4+}$  ions,<sup>1,3,25,5,16</sup> and the indications of previous band structure calculations.<sup>21,22,26</sup> In Section II we introduce this generic model for  $\text{Tl}_2\text{Mn}_2\text{O}_7$ , and make a brief presentation of the mean-field treatment that we have employed in our study. Section III exhibits the results which we obtained for different sets of parameters, including those that have been suggested by various authors<sup>25,26,16</sup> as possibly relevant for the description of this compound. A comparison is also made with the electronic structure obtained before using the IVM model,<sup>23</sup> discussing the similar features which it has been possible to exhibit between them. In Section IV a summary of our study of the HS model, and comments on the present status of the understanding of the pyrochlore compound  $\text{Tl}_2\text{Mn}_2\text{O}_7$  are presented.

## II. A MODEL FOR $\text{Tl}_2\text{Mn}_2\text{O}_7$ INCLUDING HUND AND SUPEREXCHANGE COUPLINGS

In this section we introduce a generic model for  $\text{Tl}_2\text{Mn}_2\text{O}_7$  based on the suggestions presented by many researchers,<sup>1,3,5,25,26,16</sup> general enough to allow us to make a comparative study between the various proposals which it includes as particular cases. The generic model takes into account the now widely accepted fact that in this material transport and magnetism seem to be primarily related to different electronic orbitals,<sup>3,13,19,12,20</sup> which we describe by two bands of different character which are hybridized. One band is mainly

itinerant, and the other includes strong correlations, as we now describe. The correlated electrons appear forming a lattice of local magnetic moments, and also occupying a narrow band, which are coupled via a strong Hund exchange interaction. This would correspond to the assumption that the local magnetic moments present in the material are due to  $\text{Mn}^{4+}$  ions, with occupied  $\text{Mn-}t_{2g}$  orbitals which, however, due to their mixing with O orbitals below the Fermi level, are not completely localized, giving rise to the narrow band. A hybridization exists between the correlated band and the mostly itinerant one, which is connected with the low lying conduction states involving  $\text{Tl-}6s$  orbitals and O levels (eventually hybridized with the mostly empty  $\text{Mn-}e_g$  orbitals<sup>16</sup>) in accordance with most experimental suggestions mentioned above, band structure calculations,<sup>22,26</sup> and the recent description of the pressure dependence of  $T_c$  for various CMR pyrochlores.<sup>16</sup> The possibility of a superexchange coupling between the localized spins being present is also considered.<sup>1,3,25,26,16</sup>

Concretely, the generic model that we have studied is described by the Hamiltonian

$$H = H_c + H_d + H_V + H_S, \quad (1)$$

where:

$$\begin{aligned} H_c &= -t_c \sum_{\langle i,j \rangle \sigma} (c_{i\sigma}^\dagger c_{j\sigma} + \text{H.c.}) - \mu \sum_{i\sigma} c_{i\sigma}^\dagger c_{i\sigma}, \\ H_d &= -t_d \sum_{\langle i,j \rangle \sigma} (d_{i\sigma}^\dagger d_{j\sigma} + \text{H.c.}) + (\varepsilon_d - \mu) \sum_{i\sigma} d_{i\sigma}^\dagger d_{i\sigma}, \\ H_V &= V \sum_{i\sigma} (c_{i\sigma}^\dagger d_{i\sigma} + d_{i\sigma}^\dagger c_{i\sigma}), \\ H_S &= -J_H \sum_i \mathbf{S}_i \cdot \mathbf{s}_i^{(d)} - J_S \sum_{\langle i,j \rangle} \mathbf{S}_i \cdot \mathbf{S}_j. \end{aligned} \quad (2)$$

In this Hamiltonian  $H_c$  describes the band associated to the weakly (here simplified as un-) correlated carriers in  $\text{Tl}_2\text{Mn}_2\text{O}_7$ , characterized by a hopping parameter  $t_c$  between nearest neighbors, and a creation operator  $c_{i\sigma}^\dagger$  for an electron with spin  $\sigma$  in the respective Wannier orbital centered on site  $i$ .  $H_d$  describes the narrow band associated to the correlated orbitals, characterized by a hopping parameter  $t_d$ , and a creation operator  $d_{i\sigma}^\dagger$  for an electron with spin  $\sigma$  in the Wannier orbital of reference energy  $\varepsilon_d$  (with respect to the center of the

$c$  band) localized on site  $i$ . The chemical potential of the system is denoted by  $\mu$ , and is determined by the total electronic filling  $n$ . The following term of the Hamiltonian describes a hybridization,  $H_V$ , between the  $c$  and  $d$  electron bands, which we assume to be local, for simplicity.

The last term of the Hamiltonian,  $H_S$ , describes the Hund (or Kondo-like) coupling  $J_H$  between the localized spins  $\mathbf{S}_i$  (which would represent the spin operator associated to a  $\text{Mn}^{4+}$  ion at site  $i$ , for example) and the itinerant spins, denoted by  $\mathbf{s}_i^{(d)}$ , corresponding to the narrow  $d$  band associated to the correlated electron orbitals related to Mn in  $\text{Ti}_2\text{Mn}_2\text{O}_7$ . A Heisenberg exchange term is also included in the spin Hamiltonian  $H_S$  to allow for a superexchange interaction  $J_S$  effective between the local moments of nearest neighbor Mn ions. The sign convention was chosen such that any positive spin coupling constant describes a ferromagnetic (FM) interaction, while negative ones will denote antiferromagnetic (AF) coupling.

To study the magnetic phase diagram and electronic structure of the system described by the general Hamiltonian introduced above [hereafter to be denoted also as the Hund-superexchange (HS) model], we have employed the mean field approximation as briefly discussed below.

### A. Ferromagnetic phase

We investigated the existence of a uniform ferromagnetic phase, introducing two order parameters to characterize it:

$$M = \langle S_i^z \rangle, \quad (3)$$

$$m = \langle s_i^{(d)z} \rangle \equiv \frac{1}{2} \langle d_{i\uparrow}^\dagger d_{i\uparrow} - d_{i\downarrow}^\dagger d_{i\downarrow} \rangle, \quad (4)$$

denoting by  $\langle O \rangle$  the thermal (quantum) average of operator  $O$  in the system at temperature  $T$  ( $T = 0$ , for the system in its ground state).

The corresponding mean-field Hamiltonian, after Fourier transforming the band terms, takes the form



$$\begin{aligned}
H_F^{\text{MF}} = & \sum_{\mathbf{k}\sigma} \left[ \tilde{\epsilon}_c(\mathbf{k}) n_{\mathbf{k}\sigma}^c + \tilde{\epsilon}_{d\sigma}(\mathbf{k}) n_{\mathbf{k}\sigma}^d \right] + V \sum_{\mathbf{k}\sigma} \left( c_{\mathbf{k}\sigma}^\dagger d_{\mathbf{k}\sigma} + d_{\mathbf{k}\sigma}^\dagger c_{\mathbf{k}\sigma} \right) \\
& - \sum_i (J_H m + z J_S M) S_i^z + J_H M m N + \frac{1}{2} N z J_S M^2,
\end{aligned} \tag{5}$$

where the Hund and Heisenberg exchange couplings have been decoupled as usual in mean field approximation.  $N$  stands for the total number of lattice sites,  $z$  is the coordination number, and we have defined

$$\begin{aligned}
\tilde{\epsilon}_c(\mathbf{k}) & \equiv \epsilon_{\mathbf{k}}^c - \mu, \\
\tilde{\epsilon}_{d\sigma}(\mathbf{k}) & \equiv \epsilon_{\mathbf{k}}^d - \mu - \sigma J_H M / 2,
\end{aligned} \tag{6}$$

in terms of the dispersion relations for the bare  $c$  and  $d$  bands,  $\epsilon_{\mathbf{k}}^c = -t_c \sum_{\boldsymbol{\delta}} e^{-i\mathbf{k} \cdot \boldsymbol{\delta}}$  and  $\epsilon_{\mathbf{k}}^d = \varepsilon_d - t_d \sum_{\boldsymbol{\delta}} e^{-i\mathbf{k} \cdot \boldsymbol{\delta}}$ , where  $\boldsymbol{\delta}$  describes the vectors connecting any one lattice site with its  $z$  nearest neighbors, and  $n_{k,\sigma}^\alpha \equiv \alpha_{k,\sigma}^\dagger \alpha_{k,\sigma}$ , with  $\alpha = c, d$ ;  $\sigma = \uparrow, \downarrow$ .

The first two terms on the RHS of Eq. (5) describe two hybridizing bands, one of them subject to an effective magnetic field [through the product  $J_H M$  appearing in  $\tilde{\epsilon}_{d\sigma}(\mathbf{k})$ , Eq. (6)]. The third term corresponds to an array of independent localized spins in the effective field arising from their original mutual interaction as well as their interaction with the  $d$ -band electrons. Finally, the last terms are additive constants produced by the mean-field decoupling.

The band part of the mean-field Hamiltonian  $H_F^{\text{MF}}$  is easily diagonalized, yielding the energy eigenvalues

$$E_{\pm}^\sigma(\mathbf{k}) = \frac{1}{2} \left[ \tilde{\epsilon}_c(\mathbf{k}) + \tilde{\epsilon}_{d\sigma}(\mathbf{k}) \pm \sqrt{[\tilde{\epsilon}_c(\mathbf{k}) - \tilde{\epsilon}_{d\sigma}(\mathbf{k})]^2 + 4V^2} \right], \tag{7}$$

which represent the ferromagnetic bands for spin  $\sigma$ . The corresponding eigenvectors allow us to write the electron operators of the  $c$  and  $d$  bands as combinations of operators related to the new hybrid bands (and vice-versa), which is used in the calculation of the relevant averages.

At a given temperature  $T$ , and for a fixed total band filling  $n$ , the magnetization order parameters can be calculated self-consistently through their definitions, Eqs. (3) and (4),

while the chemical potential can be determined by the self-consistency condition for the total number of electrons occupying the ferromagnetic bands. We chose to rewrite this in terms of the original  $c$  and  $d$  band fillings (denoted  $\langle n_c \rangle$  and  $\langle n_d \rangle$ , respectively):

$$n = \langle n_c \rangle + \langle n_d \rangle . \quad (8)$$

Finally, the free energy per site of the ferromagnetic solution,

$$F = F_B + F_S + F_0 , \quad (9)$$

is evaluated as the sum of three terms: the band free energy, the localized spins contribution, and additive energy constants. These terms are respectively given by

$$F_B = -T \sum_{\mathbf{k}\sigma} \sum_{\alpha=\pm} \ln \left[ 1 + e^{-E_{\alpha}^{\sigma}(\mathbf{k})/T} \right] , \quad (10)$$

$$F_S = -T \ln \text{Tr} \left[ e^{(J_H m + z J_S M) S^z / T} \right] , \quad (11)$$

$$F_0 = J_H M m + \frac{1}{2} z J_S M^2 + \mu n . \quad (12)$$

The last term in Eq. (12) must be added to compensate for the inclusion of the chemical potential in the Hamiltonian defined previously. Notice that we are dropping the Boltzmann constant, which implies that temperature will be expressed in the same units as energy.

## B. Antiferromagnetic phase

We also investigated the existence of an antiferromagnetic phase. Such long-range magnetic ordering would appear frustrated in the real pyrochlore lattice, but as a first approach, we study here a simplified version of the problem on a cubic lattice. In this case, the lattice is divided into two interpenetrating equivalent sublattices with opposite magnetizations, labeled  $A$  and  $B$  respectively. By symmetry, only two order parameters which describe the sublattice magnetizations characterize this phase:

$$\langle S_i^z \rangle = \begin{cases} M, & i \in A, \\ -M, & i \in B, \end{cases} \quad (13)$$

$$\langle s_i^{(d)z} \rangle = \begin{cases} m, & i \in A, \\ -m, & i \in B, \end{cases} \quad (14)$$

where both  $M$  and  $m$  are positive-defined quantities.

The procedure used to determine the antiferromagnetic solution in mean field approximation is similar to the one presented above for the ferromagnetic phase. For completeness, we will only include here the form assumed by the mean-field Hamiltonian,  $H_{\text{AF}}^{\text{MF}}$ , written in terms of operators characterizing the two interpenetrating sublattices:

$$\begin{aligned} H_{\text{AF}}^{\text{MF}} = & -\mu \sum_{\mathbf{k}\sigma} \left( a_{\mathbf{k}\sigma}^\dagger a_{\mathbf{k}\sigma} + b_{\mathbf{k}\sigma}^\dagger b_{\mathbf{k}\sigma} \right) + \sum_{\mathbf{k}\sigma} \epsilon_{\mathbf{k}}^c \left( e^{-i\mathbf{k} \cdot \boldsymbol{\delta}_0} a_{\mathbf{k}\sigma}^\dagger b_{\mathbf{k}\sigma} + \text{H.c.} \right) \\ & + \sum_{\mathbf{k}\sigma} \left[ (\varepsilon_d - \mu - \sigma J_H M/2) A_{\mathbf{k}\sigma}^\dagger A_{\mathbf{k}\sigma} + (\varepsilon_d - \mu + \sigma J_H M/2) B_{\mathbf{k}\sigma}^\dagger B_{\mathbf{k}\sigma} \right] \\ & + \sum_{\mathbf{k}\sigma} (\epsilon_{\mathbf{k}}^d - \varepsilon_d) \left( e^{-i\mathbf{k} \cdot \boldsymbol{\delta}_0} A_{\mathbf{k}\sigma}^\dagger B_{\mathbf{k}\sigma} + \text{H.c.} \right) + V \sum_{\mathbf{k}\sigma} \left( a_{\mathbf{k}\sigma}^\dagger A_{\mathbf{k}\sigma} + b_{\mathbf{k}\sigma}^\dagger B_{\mathbf{k}\sigma} + \text{H.c.} \right) \\ & - \sum_{i=1}^{N/2} (J_H m - z J_S M) \left[ S_i^{z(A)} - S_i^{z(B)} \right] + J_H M m N + \frac{1}{2} z J_S M^2 N. \end{aligned} \quad (15)$$

Here we have introduced two-site unit cells to describe the AF lattice and used the following notation:  $d_{i\sigma} = A_{i\sigma}(B_{i\sigma})$  for  $i \in A(B)$ ;  $c_{i\sigma} = a_{i\sigma}(b_{i\sigma})$  for  $i \in A(B)$ ; explicit indication of sublattice is made for localized-spin operators;  $\boldsymbol{\delta}_0$  is a vector connecting the two sites (one belonging to each sublattice) inside a unit cell. Notice that the wave-vector sums are now performed over the reduced Brillouin zone of the AF lattice.

The determination of the self-consistent AF solution follows along the same lines as in the FM case, except that we have to obtain numerically the eigenvalues and eigenvectors of the itinerant part of the effective Hamiltonian (15), as we are now dealing with a 4x4 matrix.

### III. RESULTS AND DISCUSSION

In this section we present some of the results we have obtained for the generic HS model introduced in the previous section using many different sets of parameters: including those which have been suggested by various authors<sup>22,25,26,16</sup> as possibly relevant for the description

of  $\text{Ti}_2\text{Mn}_2\text{O}_7$ . We want to stress that even with the simplifications adopted in the present treatment, notwithstanding the known over-estimation of critical temperatures and other limitations to be mentioned, which are inherent to the mean-field approximation used, it is nevertheless interesting to be able to exhibit features in common with the different models that have been proposed for  $\text{Ti}_2\text{Mn}_2\text{O}_7$  if appropriate relevant sets of parameters are chosen. This will be the aim of the presentation of results and discussion in this section.

For simplicity and without much loss of generality, we assume the localized spins to have  $S = 1/2$ . In this case, the mean-field self-consistency equations for the magnetization order parameter  $M$  [Eqs. (3) and (13), respectively], assume the simple form

$$M = \frac{1}{2} \tanh \left[ \frac{1}{2T} (J_H m \pm z J_S M) \right], \quad (16)$$

where the upper (lower) sign corresponds to the ferromagnetic (antiferromagnetic) solution.

We have assumed a three-dimensional simple cubic lattice ( $z = 6$ ), and used a semi-elliptic approximation for the bare densities of states (DOS). The  $c$  band half-bandwidth  $W = zt_c$  is used as the energy unit. To fix ideas in the following discussion we will choose that value to be  $\simeq 1$  eV, in qualitative agreement with experiments and band-structure calculations.<sup>22,26</sup> We also consider anti-homotetic bands, i.e.,  $t_d = -\alpha t_c$ ,  $\alpha$  being a (positive) narrowing factor. This would be consistent with an electron-like  $c$  band related to the mobile carriers,<sup>1,22,26</sup> and a narrower hole-like  $d$  band.<sup>26,22</sup>

We have investigated the existence of magnetically ordered solutions for many sets of parameters of the HS model. Both FM and AF solutions are obtained at low temperatures for wide ranges of parameter values. This puts into evidence a strong competition between these two kinds of ordering in the model. We select the physically relevant solution in each case by comparing the free energies and choosing the lowest one. In this paper we present ground-state phase diagram results (at temperatures much lower than the critical ones for either magnetic phase,  $T \ll T_{c(F)}, T_{c(AF)}$ , where full spin polarization has been established) for which the bare  $d$  band has been centered at an energy  $\varepsilon_d = -0.7$  eV (the bare  $c$  band being centered at the origin). This is consistent with the  $d$  band lying near the bottom of

the  $c$  band, which will yield a small number of conduction electrons. Our phase diagrams are plotted as functions of the bandwidth ratio  $\alpha$  and the superexchange-coupling strength  $J_S$ . In each phase diagram the following remaining parameters have been fixed: the Hund-coupling strength  $J_H$  (kept at a large value, comparable to the width of the conduction band), the hybridization  $V$  and the total electron filling  $n$ .

A fact worth noticing is a symmetry manifest in the mean-field Hamiltonians (Eqs. (5) and (15), respectively): the system is invariant under a simultaneous change of sign of the Hund-coupling  $J_H$  and of the relative orientation between magnetizations  $m$  and  $M$ . Thus, the system will not distinguish energetically between a situation corresponding to a FM-like Hund-coupling, in which case the magnetizations  $M$  and  $m$  will be parallel, and the case of AF-like Hund coupling, in which these two magnetizations would have relative anti-parallel orientations. Taking this symmetry into account, one can restrict the analysis to positive  $J_H$ , as expected on physical grounds for this compound.

We present phase-diagrams obtained for a range of electron fillings around  $n = 1$ , near the region of interest for the description of  $\text{Ti}_2\text{Mn}_2\text{O}_7$  as will be discussed shortly in connection with the electronic structure and occupation of the bands.

First, we will discuss the phase-diagrams obtained including an antiferromagnetic superexchange (SE) coupling between nearest neighbor spins, as some authors<sup>5,26</sup> have suggested:  $J_S \leq 0$ . We can make a few general statements:

i) for small enough hybridization (e.g.  $V = 0.02 \text{ eV}$ ) no ferromagnetism is obtained for any finite value of AF-superexchange in the large region of variation of the bandwidth ratio  $\alpha$  investigated ( $0 \leq \alpha \leq 0.5$ ) for fillings around  $n = 1$ ;

ii) at larger hybridization values (e.g.,  $V = 0.2, 0.3, 0.4 \text{ eV}$ ) an interesting competition between AF and F is obtained as a function of the parameters, including reentrant behavior as a function of  $\alpha$ . Though antiferromagnetism widely dominates for  $n = 1$ , we also found that for weak AF-superexchange,  $-0.01 \text{ eV} \leq zJ_S \leq 0$ , pockets of ferromagnetism appear at small to intermediate values of  $\alpha$ . In Fig. 1(a) we show how these FM pockets shift to larger  $\alpha$  values if the hybridization is increased.

Larger electron fillings [see Fig. 1(b)] increase the size of the ferromagnetic regions, which are now obtained also at smaller  $\alpha$  values (narrower bare  $d$  band). To exemplify the dependence of the phase diagram with electron filling at fixed hybridization we include Fig. 2 corresponding to hybridization  $V = 0.3$  eV, where the cases  $n = 1, 1.09, 1.15$  are shown. The effect of filling on the phase diagram is amplified for larger hybridization values.

Thus, varying the filling, in the presence of a hybridization large enough, and for a  $d$  band relatively narrower than the  $c$  band, we have demonstrated that ferromagnetism can be obtained from the HS model even in the presence of a (weak) AF-superexchange ( $J_S \leq 0$ ), as has been suggested before,<sup>26</sup> the stability region growing with increasing hybridization.

If the phase diagram in the presence of a weak FM superexchange interaction ( $J_S > 0$ ) is now investigated, as proposed early on for this compound by many researchers,<sup>1-3,22,25</sup> and later claimed to be effectively the case if a careful consideration of the effect of O-orbitals was undertaken,<sup>16</sup> of course the ferromagnetic phase is favored. Now much larger ranges of the bandwidth ratio  $\alpha$  correspond to ferromagnetic ground states, as can be appreciated in Figs. 1 and 2.

The subtle interplay of the different parameters which has been shown to determine the magnetic ordering in the HS model, in particular needed to obtain a ferromagnetic ground state for example, can be quite easily understood if one analyzes the corresponding electronic band structure. As seen in Fig. 3, where we plot the density of states decomposed in terms of the original bands, we find that for the parameter ranges in which ferromagnetism is clearly stable for the HS model, strong spin differentiation exists in the electronic structure. A band gap connected to the majority-spin orbitals is present at the Fermi level ( $E_F$ ), while a finite density of states at  $E_F$  is obtained mainly for the minority-spin conduction band  $c_{\downarrow}$ . For the fillings which have been discussed above, the chemical potential of the system is located near a hybridization band gap edge (see Fig. 3), providing occupation of the different orbitals in qualitative agreement with previous electronic structure calculations.<sup>22,26</sup> These results are also interesting as they place us in an analogous scenario to that proposed in 1997 for this compound,<sup>23</sup> when the IVM for  $\text{Ti}_2\text{Mn}_2\text{O}_7$  was introduced and shown to provide an

explanation for the results obtained in Hall experiments and the colossal nature of the MR of the compound. The presence of the Fermi level near band edges, e.g. of a hybridization gap or pseudogap, in a strongly spin differentiated electronic band structure, and especially the spin-dependent conduction band changes predicted as a function of temperature and magnetic field, were shown<sup>23</sup> to originate drastic changes in the carrier concentration around  $T_c$  which, in the absence of anomalous Hall contributions, could be directly related to the measurements in Hall experiments<sup>1</sup> and explain them. The validity of the Hall data analysis performed in Ref. 23 has recently been confirmed by new experimental reports on Hall and thermopower data over wider temperature and magnetic field ranges.<sup>14</sup> In Ref. 14 the new Hall data are successfully explained using the same approach of Ref. 23, and support the prediction of drastic carrier density changes near  $T_c$ , related to conduction band changes due to the development of magnetization, as being the main sources for the observed magnetotransport properties.<sup>23,14,17</sup>

Due to the simple mean-field approximation adopted, only at low temperatures, when the system is fully polarized, are our phase diagram results trustful, and the electronic structure results suitable for comparison with those obtained before using the IVM.<sup>23</sup> The effect of spin-polarization by the Hund interaction is not correctly estimated here at higher temperatures, being included only through the mean field magnetization order parameters. In fact, an investigation of the critical temperatures obtained here also evidenced problems related to the inability of the MFA employed to treat adequately the strong Hund correlations: the Curie temperatures obtained are found to decrease as hybridization is increased (which one would tend to connect with negative pressure coefficients for  $T_c$  as experimentally observed<sup>5,15,16</sup>) even in cases for which the phase diagrams show a stabilization of ferromagnetic ordering with increase of the hybridization (as we obtain for fillings  $n > 1$ ). This seems caused by a spurious tendency to stabilize a local magnetization due to the mutual interaction between the localized spins and the  $d$  electrons through their Hund coupling, irrespective of the intersite interactions, due to the mean field approximation employed. Thus, the shortcomings of the present treatment for all but the lowest temperatures prevent us

from addressing here the interesting issue of the ability of the HS model to describe the effect of pressure on  $T_c$  for different values of its parameters. The increase of spin disorder with temperature, and in particular the paramagnetic phase, should be much better described using the coherent potential approximation as in Ref. 23 for the IVM. We expect that such a treatment for the paramagnetic phase of the Hund-superexchange model would allow us to exhibit similarities with the IVM electronic structure results above  $T_c$ , like those shown to exist for the ferromagnetic phase in the present work, and to address other issues of interest outside the scope of the simple treatment presented in this work.

#### IV. SUMMARY

Increasing experimental evidence on magnetotransport in  $\text{Tl}_2\text{Mn}_2\text{O}_7$  points towards drastic changes in the carrier concentration around  $T_c$  as being mainly responsible for its colossal magnetoresistance. The absence of anomalous contributions to the Hall resistance has also recently been confirmed.<sup>14</sup> Since the nature of the carriers involved in magnetotransport has been established as free electron-like, there are now strong indications in favor of a direct relationship between drastic changes in the conduction band structure around  $T_c$  and the observed magnetotransport properties.

A strongly spin-differentiated electronic band structure, with drastic changes in the conduction bands around the critical temperature, seems a natural way to explain such abrupt carrier concentration changes. The presence of hybridization gaps or pseudogaps which, depending on the spin orientation of the carriers, might change drastically at  $T_c$  would allow for such a scenario.

The present paper is a first approach to show how such a scenario, first proposed for  $\text{Tl}_2\text{Mn}_2\text{O}_7$  in 1997 in connection with an intermediate valence model (IVM) introduced to describe CMR and Hall data of the compound,<sup>23</sup> can effectively also be realized starting from different microscopic models suggested for  $\text{Tl}_2\text{Mn}_2\text{O}_7$ , involving Hund and superexchange magnetic couplings, as well as hybridization effects.<sup>1-3,22,25,26,16</sup> We have performed a



detailed study of the stability of magnetically ordered phases obtained at low temperatures for various sets of parameters of a generic Hund-superexchange model (HS). The model is based on the assumption that the Mn orbitals, besides providing localized magnetic moments, also show some degree of delocalization through hybridization with the other orbitals, thus yielding a narrow band strongly coupled to the localized moments via a Hund coupling. This narrow band also shows strong hybridization with a broader conduction band, related to the carriers in the compound. The possibility of a superexchange interaction between the localized spins is also allowed for in the generic model, thereby including many of the proposals presented before for this compound. The electronic structure of the HS model was also investigated, obtaining for the ferromagnetic case a strong spin differentiation and the presence of a minority-spin metallic channel, thus exhibiting many similarities with the electronic structure derived from the IVM for this ordered phase. The simple mean-field approach adopted here is unsuitable to describe adequately the effects of the Hund interaction as temperature is increased. This limits the validity of our results to temperatures well below the critical one. It also prevents us from discussing the ability of the Hund-superexchange model to describe the pressure dependence<sup>5,15,16</sup> of  $T_c$  in its various parameter regimes.

Nowadays the mechanism responsible for the long-range ferromagnetism experimentally observed in  $\text{Tl}_2\text{Mn}_2\text{O}_7$  has not yet been conclusively identified. The results presented here, those obtained before with the IVM,<sup>23</sup> as well as the conclusions of much recent experimental work mentioned here, seem to indicate that in fact, provided the transport remains metallic, the detailed model for the magnetism matters much less than the trend with carrier density, as has been pointed out before for  $\text{Tl}_2\text{Mn}_2\text{O}_7$ .<sup>27</sup> In fact, our magnetic phase diagram results show that, although a ferromagnetic superexchange interaction between the Mn localized moments might be necessary to explain ferromagnetism in the related insulating pyrochlores (for example, where Y or Lu appear substituting Tl), the enhanced stability of FM ordering in  $\text{Tl}_2\text{Mn}_2\text{O}_7$  can be connected to the presence of spin-polarized charge carriers and hybridization effects, in accordance with previous suggestions.<sup>16,6</sup> Careful analysis of spectroscopic experiments is needed to elucidate conclusively whether the drastic changes

observed in carrier concentration are mainly related to magnetization-related changes of the conduction bands themselves and/or shifts of the conduction band edges.<sup>14,17</sup>

### ACKNOWLEDGMENTS

We especially thank Blas Alascio for enlightening discussions, and acknowledge financial support from the Argentina-Brazil cooperation program SECYT-CAPES BR/A99-EIII18/00. M.A.G. was also supported by grant PRONEX/FINEP/CNPq 41.96.0907.00 (Brazil).

## REFERENCES

- \* Member of the Carrera del Investigador Científico of CONICET (Consejo Nacional de Investigaciones Científicas y Técnicas, Argentina). C.I.V. dedicates this paper to Prof. E. Müller Hartmann, on occasion of his 60<sup>th</sup> birthday and the Festkolloquium in his honor at the Institut für Theoretische Physik zu Köln, Germany.
- <sup>1</sup> Y. Shimakawa, Y. Kubo and T. Manako, Nature 379, 55(1996); Y. Shimakawa, Y. Kubo, T. Manako, Y. V. Sushko, D. N. Argyriou, and J. D. Jorgensen, Phys. Rev. B **55**, 6399 (1997).
- <sup>2</sup> S. W. Cheong, H. Y. Hwang, B. Batlogg, and L. W. Rupp Jr., Solid State Commun. **98**, 163 (1996).
- <sup>3</sup> M. A. Subramanian, B. H. Toby, A. P. Ramirez, W. J. Marshall, A. W. Sleight, and G. H. Kwei, Science **273**, 81 (1996).
- <sup>4</sup> R. von Helmolt, J. Wecker, B. Holzapfel, L. Schultz, and K. Samwer, Phys. Rev. Lett. **71**, 2331 (1993); S. Jin, T. H. Tiefel, M. McCormack, R. A. Fastnacht, R. Ramesh, and L. H. Chen, Science **264**, 413 (1994).
- <sup>5</sup> Y. V. Sushko, Y. Kubo, Y. Shimakawa, and T. Manako, Czech. J. Phys. **46**, 2003 (1996); Y. V. Sushko, Y. Kubo, Y. Shimakawa, and T. Manako, Rev. High Pressure Sci. Tech. **7**, 505 (1998); Y. V. Sushko, Y. Kubo, Y. Shimakawa, and T. Manako, Physica B **259-261**, 831 (1999).
- <sup>6</sup> Y. Shimakawa, Y. Kubo, N. Hamada, J.D. Jorgensen, Z. Hu, S. Short, M. Nohara, and H. Takagi, Phys. Rev. B **59**, 1249 (1999).
- <sup>7</sup> H. Fujinaka, N. Kinomura, and M. Korizumi, M. Mat. Res. Bull. **14**, 1133 (1979).
- <sup>8</sup> G. H. Kwei, C. H. Booth, F. Bridges, and M. A. Subramanian, Phys. Rev. B **55**, R688 (1997).

- <sup>9</sup> A. J. Millis, P. B. Littlewood, and B. I. Shraiman, Phys. Rev. Lett. **74**, 5144 (1995); A. J. Millis, B. I. Shraiman, and R. Mueller, Phys. Rev. Lett. **77**, 175 (1996).
- <sup>10</sup> C. Zener, Phys. Rev. **82**, 403 (1951); P. W. Anderson and H. Hasegawa, Phys. Rev. **100**, 675 (1955); P. G. De Gennes, Phys. Rev. **181**, 141 (1960).
- <sup>11</sup> J. A. Alonso, M. J. Martinez-Lope, M. T. Casais, J. L. Martinez, and M. T. Fernandez-Diaz, Chemistry of Materials **12**, 1127 (2000).
- <sup>12</sup> T. Takeda *et al.*, J. Sol. State Chem. **140**, 182 (1998); B. Martinez *et al.*, Phys. Rev. Lett. **83**, 2022 (1999); R. Senis *et al.*, Phys. Rev. B **61**, 11637 (2000).
- <sup>13</sup> A. P. Ramirez and M. A. Subramanian, Science **277**, 546 (1997).
- <sup>14</sup> H. Imai, Y. Shimakawa, Y. V. Sushko, and Y. Kubo, Phys. Rev. B **62**, 12190 (2000).
- <sup>15</sup> M. Núñez Regueiro *et al.*, in *Proceedings of the MRS Meeting, Boston, 1999*.
- <sup>16</sup> M. D. Núñez-Regueiro and C. Lacroix, Phys. Rev. B **63**, 14417 (2001).
- <sup>17</sup> H. Okamura, T. Koretsune, M. Matsunami, S. Kimura, T. Nanba, H. Imai, Y. Shimakawa, Y. Kubo, preprint cond-mat/0105185.
- <sup>18</sup> J. A. Alonso *et al.*, Phys. Rev. B **60**, 15024 (1999).
- <sup>19</sup> J. A. Alonso *et al.*, Phys. Rev. Lett. **82**, 189 (1999).
- <sup>20</sup> J. A. Alonso *et al.*, Appl. Phys. Lett. **76**, 3274 (2000).
- <sup>21</sup> D. K. Seo, M. H. Whangbo, and M. A. Subramanian, Solid State Commun. **101**, 417 (1997).
- <sup>22</sup> D. J. Singh, Phys. Rev. B **55**, 313 (1997).
- <sup>23</sup> C. I. Ventura and B. Alascio, Phys. Rev. B **56**, 14533 (1997); C. I. Ventura and B. Alascio, in *Current Problems in Condensed Matter*, edited by J. L. Morán-López (Plenum Press, New York, 1998), p. 27.

<sup>24</sup> M. Uchida, H. Tanaka, M. Bartashevich, and T. Goto, preprint cond-mat/0102026.

<sup>25</sup> P. Majumdar and P. B. Littlewood, Phys. Rev. Lett. **81**, 1314 (1998).

<sup>26</sup> S. K. Mishra and S. Satpathy, Phys. Rev. B **58**, 7585 (1998).

<sup>27</sup> P. Majumdar and P. B. Littlewood, Nature **395**, 479 (1998).

## FIGURES

FIG. 1. Zero-temperature phase diagram of the HS model as a function of bandwidth ratio  $\alpha$ , and superexchange coupling  $zJ_S$ . (FM): ferromagnetic phase; (AF): antiferromagnetic phase. Parameters:  $W = zt_c = 1$  eV;  $\varepsilon_d = -0.7$  eV;  $J_H = 1.5$  eV. Phase transition lines shown for hybridizations:  $V = 0.2$  eV (solid line),  $0.3$  eV (dashed line), and  $0.4$  eV (dotted line). (a)  $n = 1$ ; (b)  $n = 1.09$ .

FIG. 2. Zero-temperature phase diagram of the HS model: dependence on filling. Same notation and parameters as in Fig. 1, except for:  $V = 0.3$  eV;  $n = 1$  (solid line),  $1.09$  (dashed line),  $1.15$  (dotted line).

FIG. 3. Ferromagnetic phase of HS model: density of states as a function of energy (measured with respect to the Fermi level, in units of  $W$ ), projected on the original bands.  $\rho_{d,\uparrow}$  (dotted line),  $\rho_{d\downarrow}$  (dot-dashed line),  $\rho_{c\uparrow}$  (dashed line),  $\rho_{c\downarrow}$  (solid line), for  $V = 0.3$  eV,  $n = 1.09$ ,  $\alpha = 0.1$ ,  $zJ_S = -0.01$  eV. Other parameters as in Fig. 1.

Fig. 1 (a) - C.I.Ventura - PRB

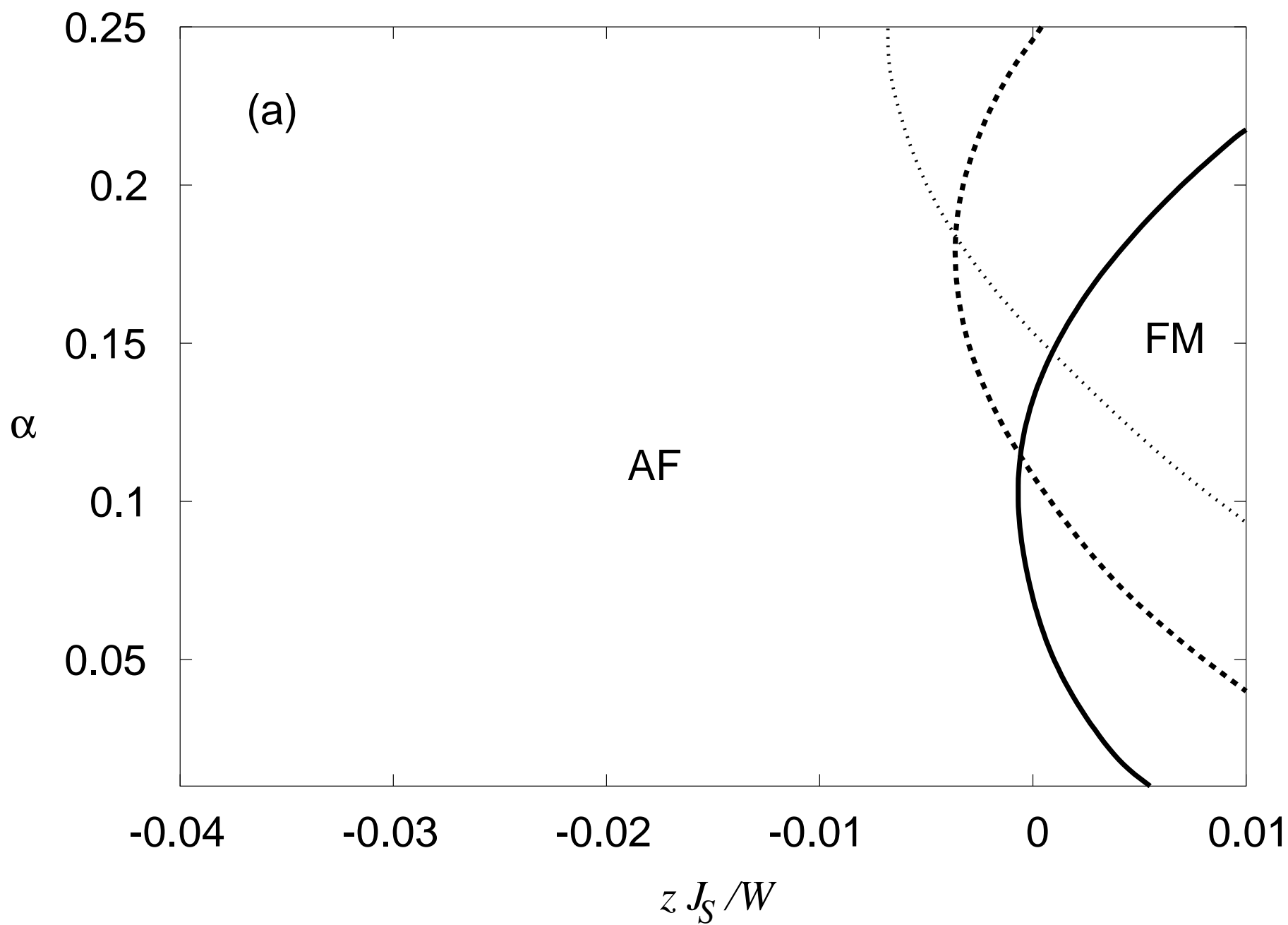


Fig. 1 (b) - C.I.Ventura - PRB

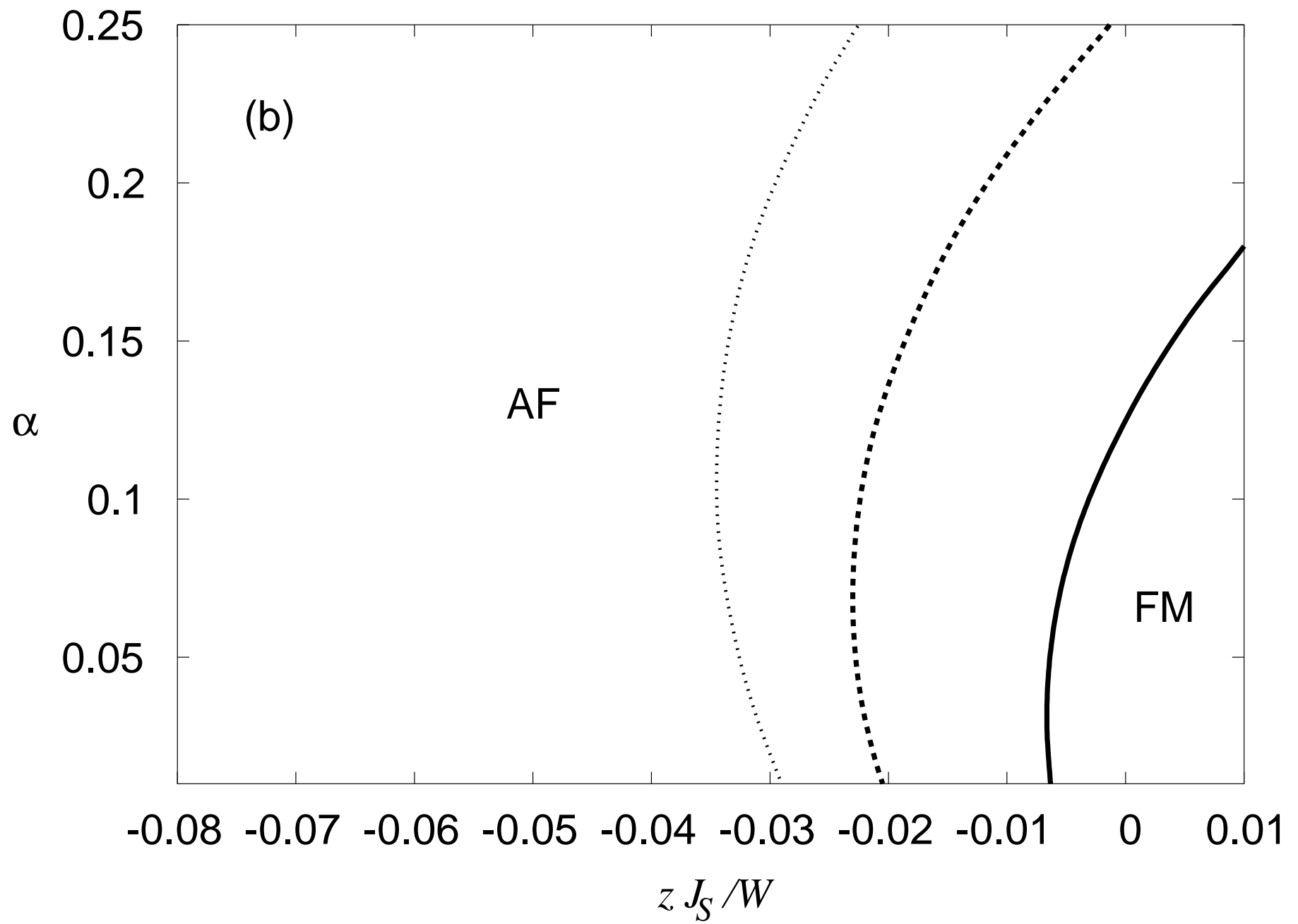




Fig. 2 - C.I.Ventura - PRB

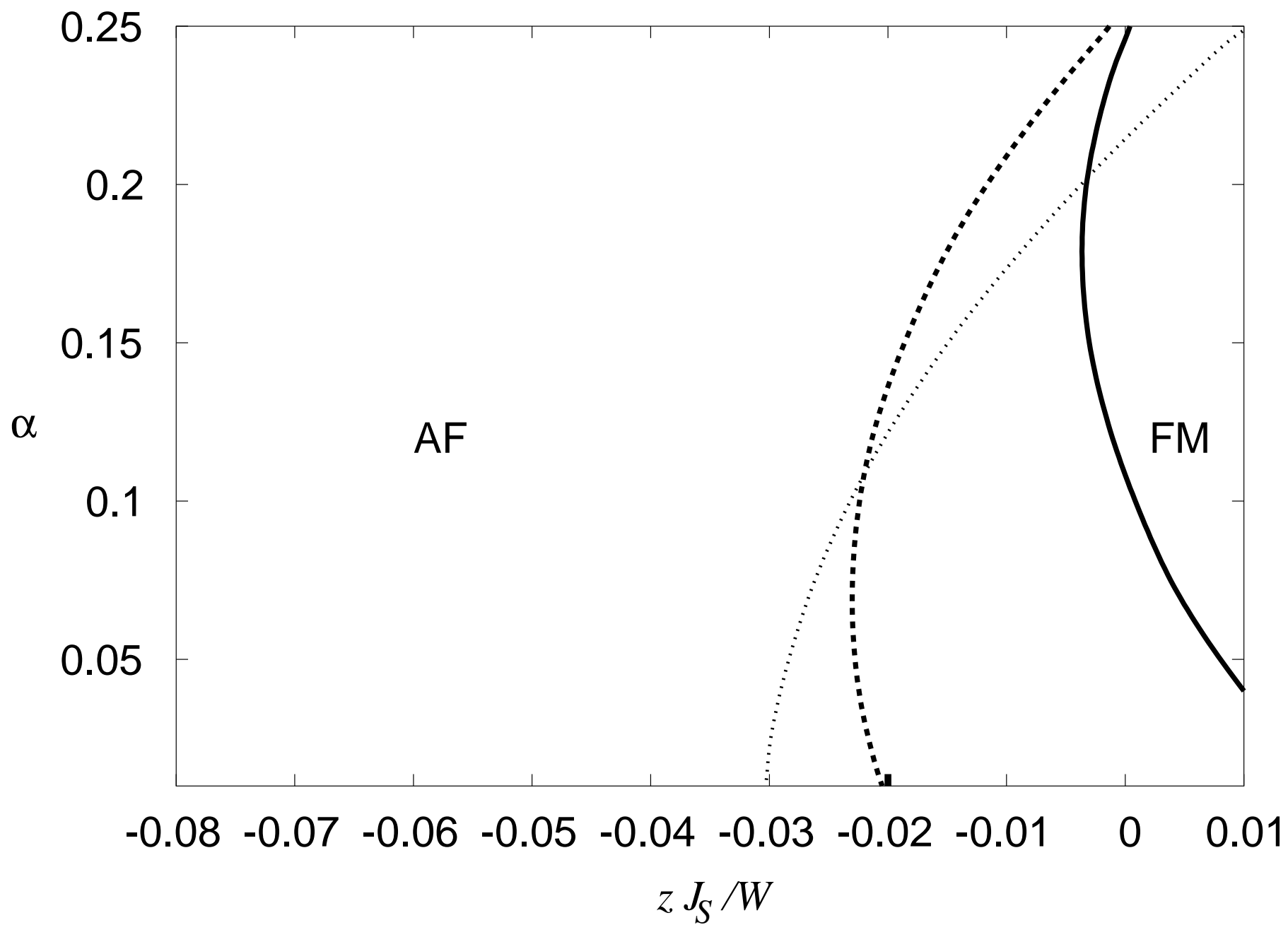


Fig. 3 - C.I.Ventura - PRB

